THE JOURNAL OF BIOLOGICAL CHEMISTRY VOL. 289, NO. 44, pp. 30785–30799, October 31, 2014


# Pigment Epithelial-derived Factor (PEDF)-triggered Lung Cancer Cell Apoptosis Relies on p53 Protein-driven Fas Ligand (Fas-L) Up-regulation and Fas Protein Cell Surface Translocation*

Received for publication, June 19, 2014, and in revised form, September 14, 2014 Published, JBC Papers in Press, September 15, 2014, DOI 10.1074/jbc.M114.590000

**Lei Li[‡§1], Ya-Chao Yao[¶1], Shu-Huan Fang[‖1], Cai-Qi Ma[‡], Yi Cen[‡], Zu-Min Xu[**], Zhi-Yu Dai[‡], Cen Li[‡], Shuai Li[‡], Ting Zhang[‡], Hong-Hai Hong[‡], Wei-Wei Qi[‡], Ti Zhou[‡], Chao-Yang Li[‡‡2], Xia Yang[‡§§3], and Guo-Quan Gao[‡¶¶4]**

*From the [‡]Department of Biochemistry, Zhongshan School of Medicine, Sun Yat-sen University, Guangzhou 510080, China, the [‡‡]State Key Laboratory of Ophthalmology, Zhongshan Ophthalmic Center, Sun Yat-sen University, Guangzhou 510060, China, the [§]Department of Reproductive Medicine Center, Key Laboratory for Reproductive Medicine of Guangdong Province, Third Affiliated Hospital of Guangzhou Medical University, 63 Duobao Road, Guangzhou 510150, China, the [¶]Laboratory Center of Guangdong No. 2 Provincial People's Hospital, Guangzhou 510317, Guangdong Province, China, the [‖]DME Center, Clinical Pharmacology Institute, Guangzhou University of Chinese Medicine, Guangzhou 510405, China, the **Cancer Center, Affiliated Hospital of Guangdong Medical College, Zhanjiang 524000, China, the [§§]China Key Laboratory of Tropical Disease Control, Sun Yat-sen University, Ministry of Education, Guangzhou 510080, China, and the [¶¶]Key Laboratory of Functional Molecules from Marine Microorganisms, Sun Yat-sen University, Department of Education of Guangdong Province, Guangdong 510080, China*

**Background:** PEDF has attracted attention for its direct antitumor effect.
**Results:** The p53-mediated cell surface translocation of Fas and up-regulation of Fas-L contributes to PEDF-induced apoptosis.
**Conclusion:** PEDF induces apoptosis by restoring the function of Fas death signaling in Fas-resistant lung cancer cells.
**Significance:** Our findings provide a potential therapeutic strategy for Fas-resistant tumors resulting from a low level of cell surface Fas.

**Pigment epithelium-derived factor (PEDF), a potent antiangiogenesis agent, has recently attracted attention for targeting tumor cells in several types of tumors. However, less is known about the apoptosis-inducing effect of PEDF on human lung cancer cells and the underlying molecular events. Here we report that PEDF has a growth-suppressive and proapoptotic effect on lung cancer xenografts. Accordingly, *in vitro*, PEDF apparently induced apoptosis in A549 and Calu-3 cells, predominantly via the Fas-L/Fas death signaling pathway. Interestingly, A549 and Calu-3 cells are insensitive to the Fas-L/Fas apoptosis pathway because of the low level of cell surface Fas. Our results revealed that, in addition to the enhancement of Fas-L expression, PEDF increased the sensitivity of A549 and Calu-3 cells to Fas-L-mediated apoptosis by triggering the translocation of Fas protein to the plasma membrane in a p53- and FAP-1-dependent manner. Similarly, the up-regulation of Fas-L by PEDF was also mediated by p53. Furthermore, peroxisome proliferator-activated receptor γ was determined to be the upstream regulator of p53. Together, these findings uncover a novel mechanism of tumor cell apoptosis induced by PEDF and provide a potential therapeutic strategy for tumors that are insensitive to Fas-L/Fas-dependent apoptosis because of a low level of cell surface Fas.**

Pigment epithelium-derived factor (PEDF),[5] a 50-kDa secreted endogenous glycoprotein, was first identified from human fetal retina pigment epithelium cell cultures as a member of the serine protease inhibitor superfamily with potent neurotropic activity (1). Since its identification, research on the biological function of PEDF has continued for decades. To date, in addition to its neurite-promoting activity, PEDF has been implicated in anti-inflammatory (2) and antiangiogenic processes (3) and in the regulation of lipid metabolism (4) and antitumor processes (5). In the context of tumors, PEDF exhibits an impressive tumor growth-suppressing activity by targeting tumor vasculature and tumor cells *per se*. Initially, the antitumor activity of PEDF was proven to be attributable to its antiangiogenic property (6). Later, increasing investigations reported that, in addition to the inhibition of angiogenesis,

* This study was supported by National Nature Science Foundation of China Grants 30971208, 30973449, 81070746, 81172163, 81272338, 81272515, 81200706, and 81400639; by National Key Sci-Tech Special Project of China Grants 2009ZX09103-642 and 2013ZX09102-053; by Program for Doctoral Station in University Grants 20100171110049, 2011M501364, and 20120171110053; by Key Project of Nature Science Foundation of Guangdong Province, China, Grant 10251008901000009; by Key Sci-tech Research Project of Guangdong Province, China, Grant 2011B031200006; by Guandong Natural Science Fund Grant 10151008901000007, S2012010009250, and S2012040006986; by Key Sci-tech Research Project of Guangzhou Municipality, China, Grants 2011Y1-00017-8 and 12A52061519; and by Changjiang Scholars and Innovative Research Team in University 985 project PCSIRT 0947.
[1] These authors contributed equally to this work.
[2] To whom correspondence may be addressed. E-mail: clioffice@yahoo.cn.
[3] To whom correspondence may be addressed. E-mail: yangxia@mail.sysu.edu.cn.
[4] To whom correspondence may be addressed: Dept. of Biochemistry, Zhongshan School of Medicine, Sun Yat-sen University, No. 74 Zhongshan 2nd Rd., Guangzhou 510080, Guangdong Province, China. Tel.: 86-020-87332128; Fax: 86-020-87332128; E-mail: gaogq@mail.sysu.edu.cn.

[5] The abbreviations used are: PEDF, pigment epithelial-derived factor; rPEDF, recombinant PEDF; Fas-L, Fas ligand; DD, death domain; DED, death effector domain; WGA, wheat germ agglutinin; PPARγ, peroxisome proliferator-activated receptor γ; PARP, poly ADP-ribose polymerase; Z, benzyloxycarbonyl; fmk, fluoromethyl ketone.

PEDF also decreases tumor proliferation by reducing tumor cell growth and/or inducing tumor cell apoptosis in a variety of tumor models, including prostate (7) glioma (8) and melanoma carcinomas (9) as well as osteosarcoma (10). Regarding lung cancer, several studies have confirmed the antitumorigenic effect of PEDF in chick embryos (11) and Lewis lung carcinoma models (12). *In vitro*, PEDF has been found to be inversely correlated with the proliferation, adhesion, and motility of A549 and SK-MES1 cells (13). However, almost nothing is known about the apoptosis-inducing effect of PEDF on human lung cancer cells and the underlying molecular events.

Fas death signaling is one of the most important extrinsic apoptosis signaling pathways that is involved in cell apoptosis. This signaling pathway is triggered through the interaction of Fas-L and Fas. By binding with Fas-L, Fas is induced to trimerize and, subsequently, recruits Fas-associated death domain, procaspase 8/10, and the caspase 8/10 regulator cellular FLICE-like inhibitory protein (c-FLIP) to assemble the death-inducing signaling complex via DED-DED and DD-DD interactions. Caspase 8 then oligomerizes and is cleaved to release from the death-inducing signaling complex, which initiates the apoptotic program (14). PEDF-induced apoptosis has been studied intensively in endothelial cells. It has been shown that PEDF can up-regulate cell surface Fas-L expression in immature endothelial cells and initiate Fas death signaling, which results in cell death (15). In addition, cPLA2-a, p38 MAPK, p53, and PPARγ have also been reported to be associated with PEDF-induced endothelial cell apoptosis (16, 17). Regarding tumor cells, PEDF-induced apoptotic cell death in the cultured non-transfected melanoma cell line G361 was blocked completely by treatment with a neutralizing antibody against Fas-L (9). Therefore, the Fas signaling pathway might play an important role in PEDF-mediated apoptosis.

Corruption of the Fas signaling pathway is frequently found in cancer. Alterations of this pathway have been proposed as mechanisms by which tumor cells can escape from apoptosis and immune system destruction (14). Mutations in the Fas gene (18), changes in the Fas intracellular signaling pathways, and the down-regulation of cell surface Fas protein (19) are the main reasons for resistance to apoptosis in a variety of human tumor cells. Several studies have reported that frequent lack of cell surface Fas expression is present in various types of lung cancer cell lines, for example, in A549 (20), H720, and H69 cells (21). It remains unclear whether PEDF can correct the deficiency of Fas death signaling in lung cancer cells so that the tumor cells regain the ability to undergo apoptosis.

In this study, we sought to investigate the direct effect of PEDF on lung carcinoma both *in vivo* and *in vitro* and focused particularly on the possible related molecular mechanisms. Here we report that PEDF can directly induce lung cancer cell apoptosis both *in vivo* and *in vitro*. Moreover, the p53-mediated translocation of Fas to the plasma membrane, which restored the function of Fas death signaling, was involved in PEDF-induced apoptosis.

## EXPERIMENTAL PROCEDURES

### Cell Lines and Animals

The human lung adenocarcinoma cell lines A549 and Calu-3 were obtained from the Cell Bank of the Chinese Academy of Sciences, where they were authenticated. The human lymphoma cell line Jurkat was provided by Prof. Tongyu Lin (Sun Yat-Sen University Cancer Center, China). The A549 and Calu-3 cells were cultured in RPMI 1640 medium (Invitrogen) containing 10% FBS (Invitrogen) and 1% penicillin/streptomycin (Invitrogen). The Jurkat cells were maintained in DMEM (Invitrogen) supplemented with 10% FBS and 1% penicillin/streptomycin. All cells were incubated at 37 °C in a humidified incubator at 5% $CO_2$. Male 4-week-old BALB/c nu/nu mice weighing 18–20 g were purchased from Guangzhou University of Chinese Medicine, China (animal license no. 20080020). All animals were maintained under specific pathogen-free conditions in the Laboratory Animal Center of Sun Yat-sen University.

### Reagents

The Attractene and HiPerFect transfection reagents were obtained from Qiagen (Carson City, CA). Anti-Fas antibody (CH-11), caspase 9 inhibitor I (Z-LEHD-fmk) and caspase inhibitor I (Z-VAD-fmk) were purchased from Merck Millipore (La Jolla, CA). Caspase 8 inhibitor II (Z-IETD-fmk) and antibodies for anti-β-actin and anti-GAPDH were obtained from Sigma-Aldrich (St. Louis, MO). Wheat germ agglutinin (WGA) conjugated to Texas Red-X and a secondary antibody conjugated to Alexa Fluor 488 and DAPI were from Invitrogen. The anti-PEDF polyclonal antibody was a gift from Prof. Jianxing Ma (Medical University of South Carolina). Antibodies for caspase 8/9 and PARP were purchased from Cell Signaling Technology. Purified mouse anti-human CD178 (Fas-L), FITC mouse anti-human CD95 (Fas), and FITC mouse IgG1 κ isotype control antibodies were obtained from BD Biosciences. Anti-PPARγ, anti-Fas, and anti-FAP-1 antibodies were from Santa Cruz Biotechnology. Anti-Phospho-p53 (Ser-15) and anti-p53 antibodies were purchased from Beyotime Institute of Biotechnology (Shanghai, China). Recombinant human endostatin injections (ENDOSTAR) were obtained from Shandong Simcere-Medgenn Bio-Pharmaceutical Co., Ltd.

### Plasmids and siRNAs

The plasmids pcDNA3.1 (+) vector and PEDF-pcDNA3.1 (+) were maintained by our own laboratory. The Fas-L and p53 cDNAs were isolated from A549 cell RNA and cloned into pBiFC-VC155 (provided by Dr. Changdeng Hu, Purdue University) and pcDNA3.1 (+) expression vectors, respectively. The primer sequences of Fas-L and p53 were as follows: Fas-L, 5′-CCGGAATTCTCATGCAGCAGCCCTTCAATT-3′ (forward) and 5′-CTCCCGGAGGAGCTTATATAAGCCGAAAAACGTC-3′ (reverse); p53, 5′-CCCAAGCTTGGGATGGAGGAGCCGCAGTC-3′ (forward) and 5′-CCGGAATTCCGGTCAGTGGAGTCAGGCCC-3′ (reverse). All plasmids were purified with a NucleoBond Xtra Midi EF kit (MN, Germany) following the protocol of the manufacturer. The siRNAs for silencing p53, Fas-L, FAP-1, and PPARγ were purchased from RIBOBIO (Guangzhou, China). Scrambled siRNA (RIBOBIO) was used as a nonspecific siRNA control.

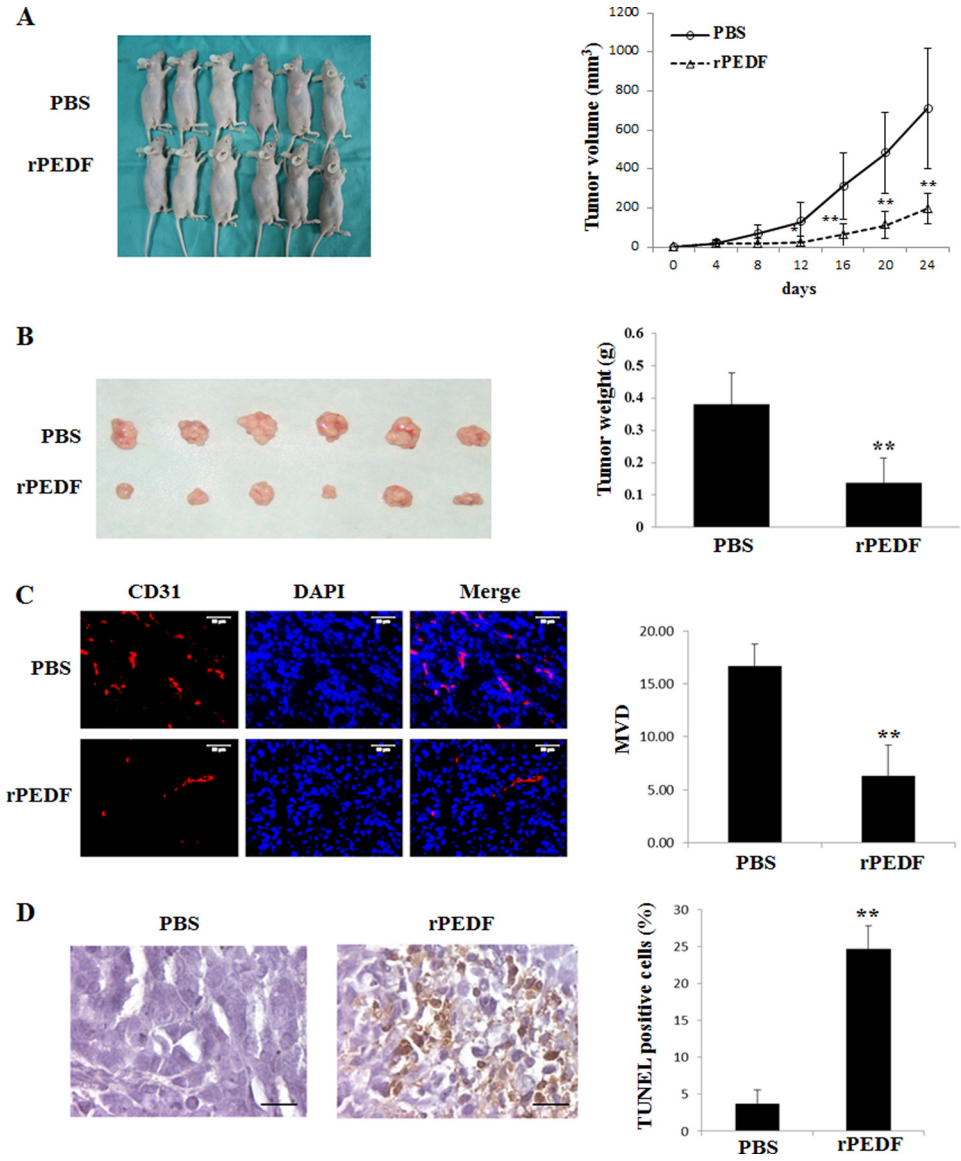


FIGURE 1. **Growth inhibition, angiogenesis repression, and apoptosis induction by rPEDF in A549 xenografts.** *A*, mice received a total of five intraperitoneal injections of rPEDF ($n = 6$, *bottom row*) or the same volume of PBS ($n = 6$, *top row*) every other day beginning on day 8 post-transplantation. On day 24 after tumor inoculation, the mice were executed and photographed. Tumor volumes were measured every 2 days and are displayed as tumor growth curves. Data are mean ± S.D. *, $p < 0.05$; **, $p < 0.01$. *B*, tumor tissues from the executed mice. *Top row*, tissues from mice treated with PBS. *Bottom row*, tissues from mice treated with rPEDF. The weights of tumor tissues served as the inputs for the statistical analysis. Data are mean ± S.D. of 6 mice/group. **, $p < 0.01$ *versus* PBS control. *C*, frozen sections of tumor tissues were subjected to immunohistochemical staining with an endothelial-specific antibody against CD31. Typical pictures of CD31-positive vessels are shown. Quantitative analysis of the CD31-positive vessels was then performed. In all samples, the mean number of microvessels was calculated from the five vascular hot spots. Data are mean ± S.D. **, $p < 0.01$ *versus* PBS control. *Scale bars* = 50 μm. *MVD*, microvessel density. *D*, representative photographs of apoptotic cells generated by TUNEL (*brown*) assay in paraffin sections of tumor tissues. The nuclei were counterstained with hematoxylin. A quantitative analysis of the apoptotic cells percentage in tumor tissues was performed. **, $p < 0.01$ *versus* PBS control. *Scale bars* = 50 μm.

### *Treatments*

*rPEDF*—rPEDF was expressed and purified as described previously (22). The culture medium was replaced with a serum-free medium containing various concentrations of rPEDF or ENDOSTAR until the cells reached 60–70% confluence. After incubation for the indicated times, the cells were harvested and used for subsequent experiments.

*Transfection*—The cells were transfected with the indicated plasmids and/or siRNA using Attractene and/or HiPerFect transfection reagents according to the instructions of the manufacturer. For the transfection of Jurkat cells, the Neon™ transfection system was used following the instructions of the manufacturer (Invitrogen). The growth medium was replaced with serum-free medium at 12 h after transduction of the PEDF and Fas-L genes. For the interference and caspase inhibitors experiments, the cells were pretreated for 12 h and 30 min prior to transfection of the PEDF gene, respectively. At the designated times, the cells were harvested and used for further experiments.

### *Cell Viability Assay*

Cells were seeded in 24-well plates in quadruplicate. After indicated treatments, the cell viability was determined by the 3-(4,5-dimethylthiazol-2-yl)-2,5-diphenyltetrazolium bromide

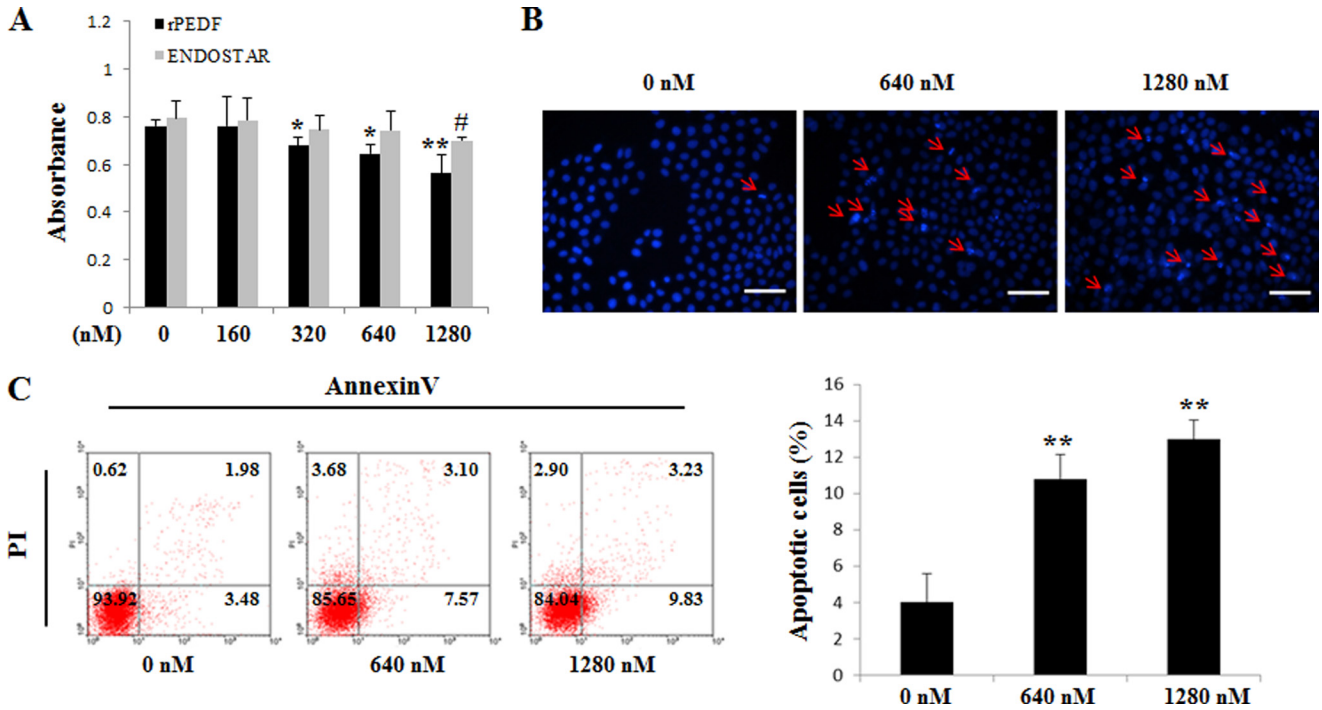


FIGURE 2. **Effects of rPEDF and ENDOSTAR on cell viability and apoptosis in A549 cells *in vitro*.** *A*, A549 cells were treated with rPEDF or ENDOSTAR at the indicated concentrations for 72 h in the absence of serum. Cell viability was determined by 3-(4,5-dimethylthiazol-2-yl)-2,5-diphenyltetrazolium bromide assay. Data represents absorbance at 570 nm and are mean ± S.D. of quadruplicates of three independent experiments. * and #, $p < 0.05$; **, $p < 0.01$ *versus* controls. *B*, cells were harvested for Hoechst staining. Cells were treated with rPEDF at concentrations of 0, 640, and 1280 nM. Representative pictures from three independent experiments photographed at ×400 are shown. Apoptotic cells were identified by chromatin condensation and nucleus fragmentation (*red arrows*). *Scale bar* = 50 μm. *C*, in parallel experiments, the samples were subjected to FITC-annexin V/propidium iodide (*PI*) staining, and a quantitative analysis of apoptotic cells was performed using flow cytometry. Diagrams of FITC-annexin V/propidium iodide flow cytometry in a representative experiment are presented as graphs. Quantifications of apoptotic cells are shown as mean ± S.D. of triplicates. *, $p < 0.05$; **, $p < 0.01$ *versus* control.

(Sigma, MO) following the protocol of the manufacturer. Absorbance was measured at 570-nm wavelength.

### *Hoechst Staining and Cell Apoptosis Analysis by Flow Cytometry*

After the indicated treatments, the cells were washed three times with PBS and fixed with 4% polyformaldehyde for 10 min at 37 °C. After another three PBS washes, the cells were subjected to Hoechst 33342 (Sigma) at a final concentration of 5 μg/ml while incubating for 30 min at room temperature in the dark. Apoptotic cells were identified by chromatin condensation and nucleus fragmentation under a fluorescence microscope. For quantitative analysis of apoptosis, the cells were prepared as described elsewhere (23). Annexin V and propidium iodide (KeyGEN BioTECH, Nanjing, China) were added for incubation in the dark for 15 min at 4 °C, and then cells were analyzed by a flow cytometer (EPICS XL-MCL or Gallios, Beckman).

### *Flow Cytometric Analysis of Cell Surface Fas Expression*

Cell surface Fas expression was determined by flow cytometry (Gallios, Beckman) according to the description by Zheng *et al.* (24). Briefly, the cells were rinsed with flow cytometry buffer (PBS containing 1% BSA and 0.05% $NaN_3$) and collected by digestion with 10 mM EDTA at 4 °C for 20 min. After washing three times, the cells were probed with either FITC-conjugated mouse anti-human CD95 (Fas) or FITC-conjugated mouse IgG1 κ isotype control antibodies (1:50) for 30 min at 4 °C in the dark and then washed again. 30,000 cells were examined for each determination.

### *Fluorescent Immunocytochemistry*

Cells embedded on glass slides were washed twice with PBS and stained with 5 μg/ml WGA for 10 min at 37 °C. After rinsing three times, the cells were fixed with 4% paraformaldehyde for 10 min at 37 °C, followed by blocking with 5% BSA for 30 min at room temperature. The Fas protein was detected using a monoclonal anti-Fas antibody (1:100) and a secondary antibody conjugated to Alexa Fluor 488 (1:200). Cell nuclei were stained with DAPI (1:2000). All slides were viewed under a confocal laser-scanning microscope (LSM710, Zeiss, Jena, Germany).

### *Western Blot Analysis*

Western blot analysis was performed as described elsewhere (25). Antibodies for caspase 8/9, PARP, Fas-L, Fas, phospho-p53, and p53 were used at 1:1000 dilution. Antibodies for β-actin and GAPDH were used at 1:10,000 dilution. The bound antibody was visualized using HRP-conjugated secondary antibodies.

### *Animal Studies*

The A549 heterotopic transplanted tumor model was established as described previously, with some modifications (22). When tumors were visible, the mice were randomly assigned to two groups with six mice in each group. One group received peritoneal injections with 5 mg/kg PEDF per mouse, whereas the other group received the same volume of PBS as a control. Mice received five injections every other day until the overall dose reached 25 mg/kg. Nude mice were weighed, and the tumor length and width diameters were measured every 2 days.

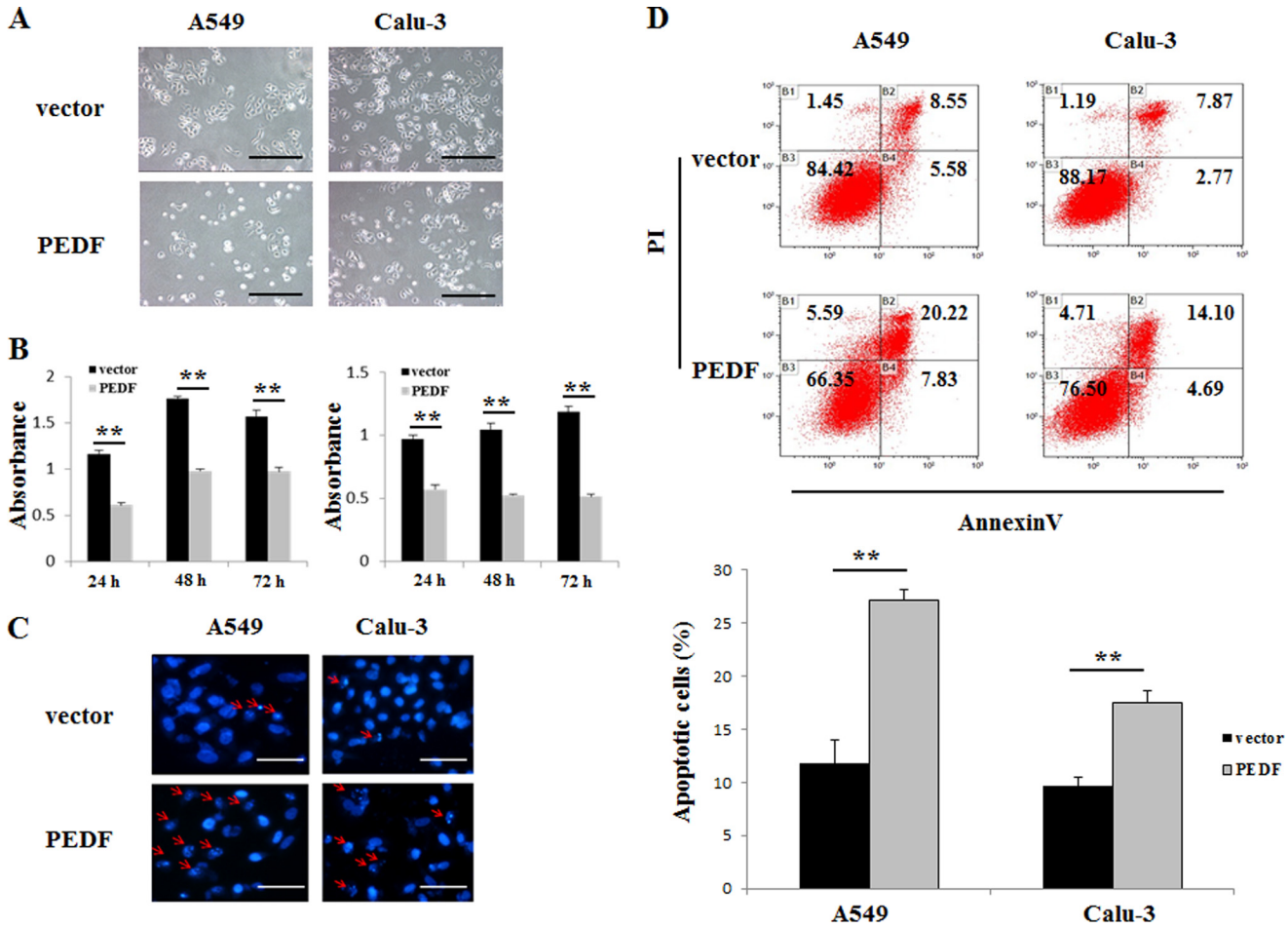


FIGURE 3. **Effects of PEDF overexpression on cell viability and apoptosis in A549 and Calu-3 cells.** *A*, typical photographs of cells transfected with vector (*top row*) or PEDF (*bottom row*) for 48 h after serum depletion. Data are representative of three independent experiments. *Scale bars* = 50 $\mu$m. *B*, 3-(4,5-dimethylthiazol-2-yl)-2,5-diphenyltetrazolium bromide assay for the viability of cells transfected with vector or PEDF for 24, 48, and 72 h after serum depletion. Data represent absorbance at 570 nm and are mean ± S.D. of quadruplicates. **, $p < 0.01$ *versus* the vector-only group. Data are representative of three independent experiments. *C*, after transduction of vector (*top row*) or PEDF (*bottom row*) for 48 h in the absence of serum, the cells were harvested for Hoechst staining. Representative pictures from three independent experiments photographed at ×200 are shown. The apoptotic cells were identified by chromatin condensation and nucleus fragmentation (*red arrows*). *Scale bars* = 200 $\mu$m. *D*, in parallel experiments, the samples were subjected to FITC-annexin V/propidium iodide staining, and a quantitative analysis of apoptotic cells was performed using flow cytometry. Diagrams of the FITC-annexin V/propidium iodide flow cytometry in a representative experiment are presented. Quantifications of the apoptotic cells are shown as mean ± S.D. of triplicates. **, $p < 0.01$ *versus* the vector-only group.

The tumor volume was determined according to the following equation: volume = (length × width$^2$) × 0.5. 24 days after the first injection of A549 cells, tumors were dissected, weighed, and stored at −80 °C for Western blot and immunohistochemistry analyses. All animal studies were performed under an institutionally approved protocol according to the USPHS Guide for the Care and Use of Laboratory Animals.

### *Microvessel Density Assay*

Frozen sections were treated with non-immune goat serum to block nonspecific binding (background). The sections were then incubated with 1:100 dilution of the rat monoclonal antibody against CD31 (BD Biosciences) at 4 °C overnight. After rinsing with PBS, the sections were subjected to the cy3-labeled goat anti-rabbit antibody (1:200) at 37 °C for 30 min. The cell nuclei were stained with DAPI (1:2000) at room temperature for 10 min. All slides were viewed under a fluorescence microscope (Axio Observer Z1, Zeiss). The tumor vasculature was quantified according to the Weidner method (26).

### *TUNEL Assay in A549 Xenografts*

Paraffin sections from each tumor were analyzed by TUNEL staining using an *in situ* cell death detection kit (Merck Millipore). A brown coloration indicated apoptotic cells. The number of apoptotic cells was counted in five randomly selected fields using a conventional optical microscope.

### *Statistical Analysis*

All data are expressed as mean ± S.D. SPSS 13.0 software was used for the one-way analysis of variance in all statistical analyses (SPSS, Chicago, IL). $p < 0.05$ was considered statistically significant.

## RESULTS

*Inhibitory Effects of PEDF on Tumor Proliferation and Angiogenesis in the Heterotopic Transplanted Human Lung Cancer Nude Mice Model*—We first investigated the antitumor activity of PEDF *in vivo*. Heterotopic xenografts of the human cell line A549 were established in the dorsi of the right front paws of

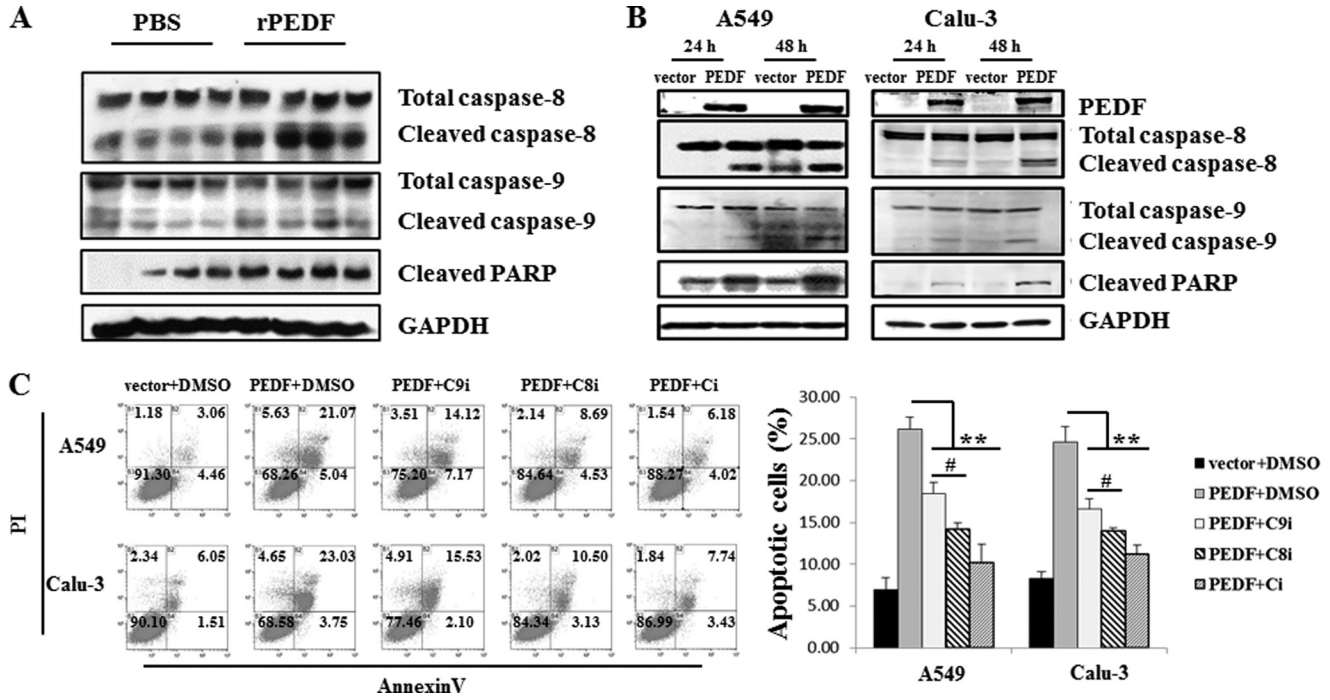


FIGURE 4. **PEDF induces the cleavage of procaspase 8/9/PARP *in vivo* and *in vitro*.** *A* and *B*, tumor tissues (*first* through *fourth lanes*, from PBS-treated mice; *fifth* through *eighth lanes*, from rPEDF-treated mice) (*A*) and cell lysates (*B*) were subjected to Western blot analysis. The protein levels of caspase 8/9/PARP were detected. *C*, the effects of caspase inhibitors on PEDF-triggered apoptosis were quantified by flow cytometry using annexin V and propidium iodide (*PI*) staining. A549 and Calu-3 cells were transfected with a vector or the PEDF gene for 48 h in the absence of serum or pretreated with 20 $\mu$M caspase 9 inhibitor I (Z-LEHD-fmk, *C9i*) or 20 $\mu$M caspase-8 inhibitor II (Z-IETD-fmk, *C8i*) or caspase inhibitor I (Z-VAD-fmk, *Ci*) for 1 h before PEDF transduction. Representative diagrams are shown. Data are mean ± S.D. of three independent experiments. **, $p < 0.01$ *versus* PEDF + dimethyl sulfoxide (*DMSO*)-treated cells; #, $p < 0.05$, PEDF + Z-IETD-fmk *versus* PEDF + Z-LEHD-fmk.

nude mice. Eight days after the first inoculation with A549 cells, the mice were randomly assigned into two groups that received intraperitoneal injections of PBS ($n = 6$) or rPEDF ($n = 6$). The rPEDF-treated group exhibited slower growth kinetics than the PBS-treated group, and a 72.6% reduction in tumor volumes was observed by day 24 (Fig. 1*A*). Accordingly, the mean weight of the tumors of the mice treated with rPEDF was significantly lower than that of mice that received PBS injections (Fig. 1*B*). The microvessel density assay revealed that PEDF treatment apparently reduced microvessel density compared with PBS treatment (Fig. 1*C*).

*Induction of Tumor Cell Apoptosis by PEDF in Vivo*—To evaluate whether PEDF influences tumor cell apoptosis *in vivo*, paraffin sections from each tumor tissue were analyzed using a TUNEL assay. As shown in Fig. 1*D*, the numbers of apoptotic cells in the tumor tissues of the rPEDF-treated group were increased significantly compared with those of the PBS-treated group. These data suggest that PEDF might directly target tumor cells.

*Growth and Apoptosis of Lung Cancer Cells in Vitro*—To measure the effects of PEDF on cell viability and apoptosis *in vitro*, a 3-(4,5-dimethylthiazol-2-yl)-2,5-diphenyltetrazolium bromide assay, Hoechst staining, and flow cytometry were employed. The rPEDF-treated group exhibited a dose-dependent reduction in viable cells, whereas ENDOSTAR, a commercial antiangiogenesis recombinant protein, had no effect on A549 cells up to a dose of 1280 nM (Fig. 2*A*). Moreover, rPEDF obviously induced the apoptosis of A549 cells (Fig. 2, *B* and *C*). To further establish this relationship, PEDF overexpression was performed in A549 and Calu-3 cells. We found significant reductions in cell numbers at 24, 48, and 72 h after serum depletion (Fig. 3, *A* and *B*) in PEDF-positive cells compared with vector controls. Furthermore, the proportions of apoptotic cells with characteristics of chromatin condensation and nucleus fragmentation (*red arrows*) were increased dramatically in PEDF-transfected cells (Fig. 3*C*). Consistent with Hoechst staining results, a progressive increase in apoptosis was observed via quantitative analysis by flow cytometry in PEDF-positive cells (Fig. 3*D*). These results demonstrate that PEDF directly induced the apoptosis of lung cancer cells and might therefore contribute to the blockade of tumor growth.

*PEDF-induced A549 and Calu-3 Cell Apoptosis Is Mediated Primarily by Caspase 8 Activation*—The activation of caspase 8 and caspase 9 has been shown to be involved in PEDF-induced human umbilical vein endothelial cell (HUVEC) apoptosis (17). To examine whether this process is also involved in PEDF-induced lung cancer cell apoptosis, the cleavage of caspase 8/9/PARP was detected by Western blot analysis. Both *in vivo* and *in vitro* studies demonstrated that PEDF significantly increased the levels of cleaved caspase 8/9/PARP (Fig. 4, *A* and *B*). Caspase 8 and caspase 9 have been identified as central components in the death receptor and mitochondrial apoptotic pathways, respectively (27). To further investigate which apoptosis signaling pathway was primarily responsible for the PEDF-triggered apoptosis of A549 and Calu-3 cells, the cells were pretreated with caspase 8 inhibitor II (Z-IETD-fmk), caspase-9 inhibitor I (Z-LEHD-fmk), and caspase inhibitor I (Z-VAD-

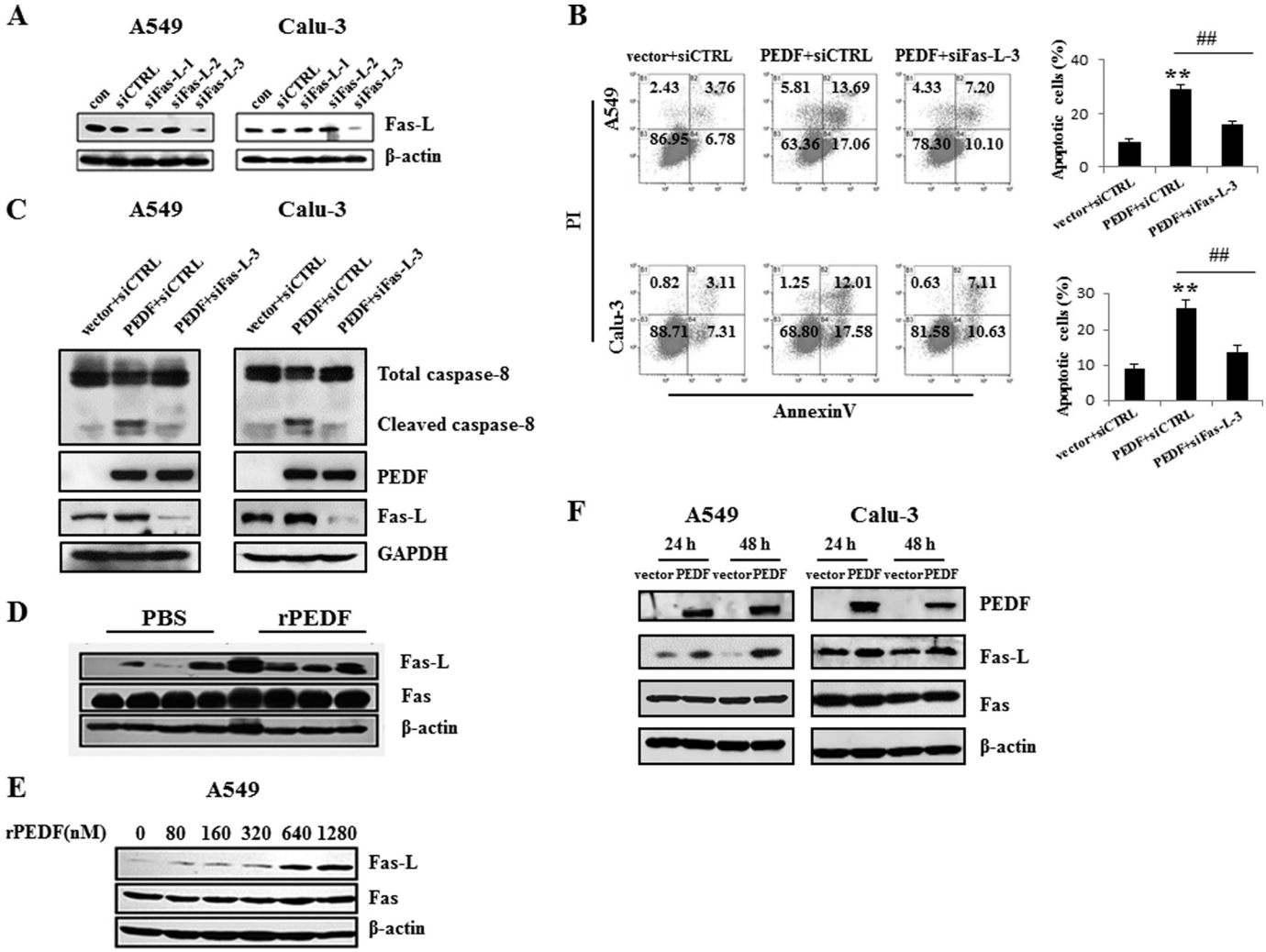


FIGURE 5. **PEDF-induced apoptosis is Fas-L-dependent.** *A–C*, after 48 h, the interference effects of the Fas-L siRNAs (*siFas-L-1/2/3*) were analyzed by Western blot analysis. Fas-L siRNA-3 (*siFas-L-3*) or nonspecific siRNA was transfected into A549 and Calu-3 cells for 12 h before PEDF gene or vector transduction. After 48 h of serum depletion, the cells were harvested for the quantification of the apoptotic cells by flow cytometry (*B*) and Western blot analysis (*C*). Representative diagrams are shown. The apoptosis results are presented as mean ± S.D. of three independent experiments. **, $p < 0.01$ *versus* vector + siCTRL-treated cells; ##, $p < 0.01$ *versus* PEDF + siCTRL-treated cells. *con*, control; *siCTRL*, control siRNA; *PI*, propidium iodide. *D–F*, the protein levels of Fas-L, but not that of Fas, were up-regulated in the tumor tissues (*first* through *fourth lanes*, from PBS-treated mice; *fifth through eighth lanes*, from rPEDF-treated mice) (*D*) or A549 cells (*E*) by rPEDF in a dose-dependent manner or by overexpression of PEDF in A549 and Calu-3 cells (*F*). Western blot analysis was employed to detect the expression of Fas-L and Fas. Data are representative of three independent experiments.

fmk). PEDF-induced apoptosis was partially blocked by pretreatment with caspase 9 inhibitor I, largely broken by caspase 8 inhibitor II, and almost completely retarded by caspase inhibitor I (Fig. 4*C*). These studies confirm that PEDF-triggered apoptosis is primarily associated with activation of caspase 8.

*PEDF Induces Fas-L-dependent Apoptosis of A549 and Calu-3 Cells*—The activation of caspase 8 commonly participates in Fas-L/Fas-mediated cell death (28). Therefore, we verified the role of Fas-L/Fas in the process of PEDF-induced apoptosis. Fas-L siRNAs were synthesized. Western blot analysis revealed that siRNA-3 specifically knocked down Fas-L in both A549 and Calu-3 cells (Fig. 5*A*). Knockdown of Fas-L by siRNA-3 abolished PEDF-induced apoptosis and caspase 8 activation (Fig. 5, *B* and *C*), which suggested that the Fas-L/Fas-mediated cell death signaling pathway played a critical role in PEDF-induced apoptosis. To elucidate how this pathway was involved, we examined the Fas-L and Fas protein levels following PEDF treatment of tumor tissues and cells. Compared with the PBS-treated group, Fas-L expression was enhanced by rPEDF injection *in vivo* (Fig. 5*C*). *In vitro*, PEDF increased the level of Fas-L in a dose-dependent manner in A549 cells (Fig. 5*D*). Consistently, Fas-L expression was also up-regulated in PEDF-transfected cells compared with vector-transfected cells (Fig. 5, *C* and *F*). However, we found no appreciable alteration of Fas in PEDF-positive cells compared with controls (Fig. 5, *D–F*). Collectively, these results established that Fas-L/Fas signaling was the primary pathway of PEDF-induced apoptosis in A549 and Calu-3 cells.

*p53 Mediates the Up-regulation of Fas-L by PEDF*—The Fas-L protein level was increased in cells transfected with p53-pcDNA3.1(+) compared with those transfected with the vector control (Fig. 6*A*). Next, we validated the influence of PEDF on p53. Overexpression of PEDF led to elevated levels of p53 and p-p53 (Ser-15) proteins (Fig. 6*B*). Knockdown of p53 diminished the effect of PEDF on the expression of Fas-L (Fig. 6, *C* and *D*).

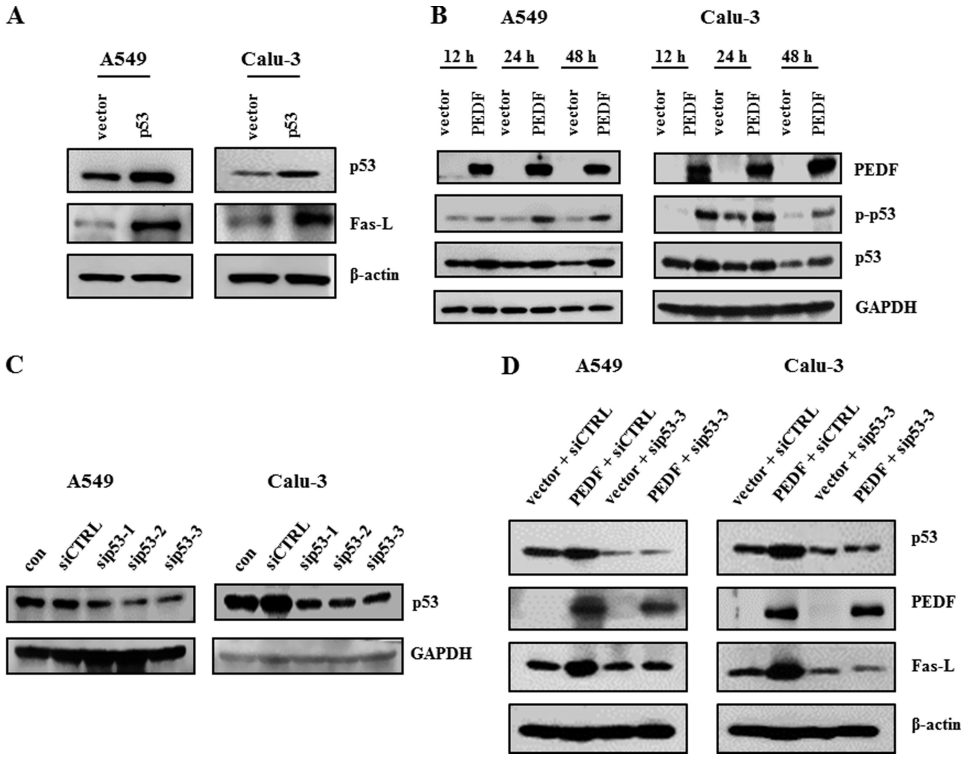


FIGURE 6. **PEDF up-regulates Fas-L expression via p53.** *A*, cells were transfected with p53-pcDNA3.1 (+) for 48 h. The protein levels of p53 and Fas-L were measured by Western blot analysis using antibodies for p53 and Fas-L, respectively. *B*, PEDF increased the expression of p53 and p-p53. The protein levels of p53 and p-p53 were detected by Western blot analysis. *C*, cells were transfected with p53 siRNAs (*sip53–1/2/3*) or a nonspecific control siRNA (*siCTRL*) for 48 h. siRNA-mediated depletion of p53 was examined by Western blot analysis. *D*, knockdown of p53 was performed 24 h prior to the overexpression of PEDF. Western blot analysis was used to determine the protein levels of p53, PEDF, and Fas-L. Data are representative of three independent experiments.

*A549 and Calu-3 Cells Were Resistant to Fas-L/Fas-mediated Apoptosis because of the Low Level of Surface Fas Protein Expression*—It has been reported that A549 cells are insensitive to Fas-L/Fas-mediated apoptosis (20). As shown in Fig. 7, *A* and *B*, the overexpression of Fas-L in A549 and Calu-3 cells failed to induce apoptosis, whereas Jurkat cells underwent apoptosis with Fas-L overexpression. Following treatment with anti-Fas antibody (CH-11), the rates of apoptosis in A549 and Calu-3 cells did not differ from those of controls, whereas Jurkat cells exhibited a marked induction of apoptosis (Fig. 7*C*). A low level of surface Fas protein expression leading to resistance to apoptosis has been reported (19). Decreased surface Fas expression has been observed in several lung cancer cell lines, including A549 cells (29). Therefore, we analyzed Fas expression on the cell plasma membrane using fluorescence immunocytochemistry and flow cytometry assays. Confocal microscopy photographs revealed that the Fas protein was nearly completely localized within the cytoplasm of A549 and Calu-3 cells. Conversely, in Jurkat cells, Fas protein was visualized on the cell plasma membrane (Fig. 7*D*). Accordingly, there was much less surface Fas protein expression in A549 (mean fluorescence intensity, 1.04) and Calu-3 (mean fluorescence intensity, 0.86) cells than in Jurkat cells, as measured by flow cytometry (mean fluorescence intensity, 2.25) (Fig. 7*E*).

*PEDF Increases Cell Surface Fas Protein in A549 and Calu-3 Cells via the p53-mediated Translocation of Fas*—Although A549 and Calu-3 cells exhibit negligible levels of cell surface Fas, Fas-L/Fas signaling was still available for PEDF-induced apoptosis. To further dissect how PEDF restored the Fas-L/Fas death receptor pathway in A549 and Calu-3 cells, we assessed the effect of PEDF gene transduction on the translocation of Fas protein. The PEDF-transfected group exhibited a marked increase of plasma membrane Fas fluorescence, as examined by confocal microscopy (Fig. 8*A*). Moreover, as measured by flow cytometry, a significant enhancement of the mean fluorescence intensity of cell surface Fas occurred in PEDF-transfected cells (Fig. 8*B*). Because p53 is involved in the trafficking of Fas (30), we determined the role of p53 in our cell model. We observed an increase in the mean fluorescence intensity of cell surface Fas in p53-overexpressing cells (Fig. 8*C*). Next, we defined the effect of p53 on the PEDF-induced translocation of Fas. Upon PEDF transfection, knockdown of p53 with siRNA-3 abrogated the PEDF-triggered increase of cell surface Fas (Fig. 8*D*). Furthermore, PEDF-induced apoptosis was also arrested by the interference of p53 (Fig. 8*E*). Taken together, our results suggest that p53 activation was critical for the PEDF-induced Fas transport to the cell surface that resulted in the apoptosis of A549 and Calu-3 cells.

*PEDF-induced Fas Transport Is Mediated by the p53/FAP-1 Axis*—To figure out the downstream regulatory factor involved in PEDF-induced Fas transport, we focused on the protein FAP-1, which is a negative regulatory molecule of Fas translocation (31). As shown in Fig. 9, *A* and *B*, the knockdown of FAP-1 increased the mean fluorescence intensity of cell surface Fas. Moreover, the overexpression of PEDF decreased FAP-1 protein levels in A549 and Calu-3 cells (Fig. 9*C*). Similarly, we found that overexpression of p53 reduced the expression of FAP-1(Fig. 9*D*). Furthermore, knockdown of p53 cancelled the

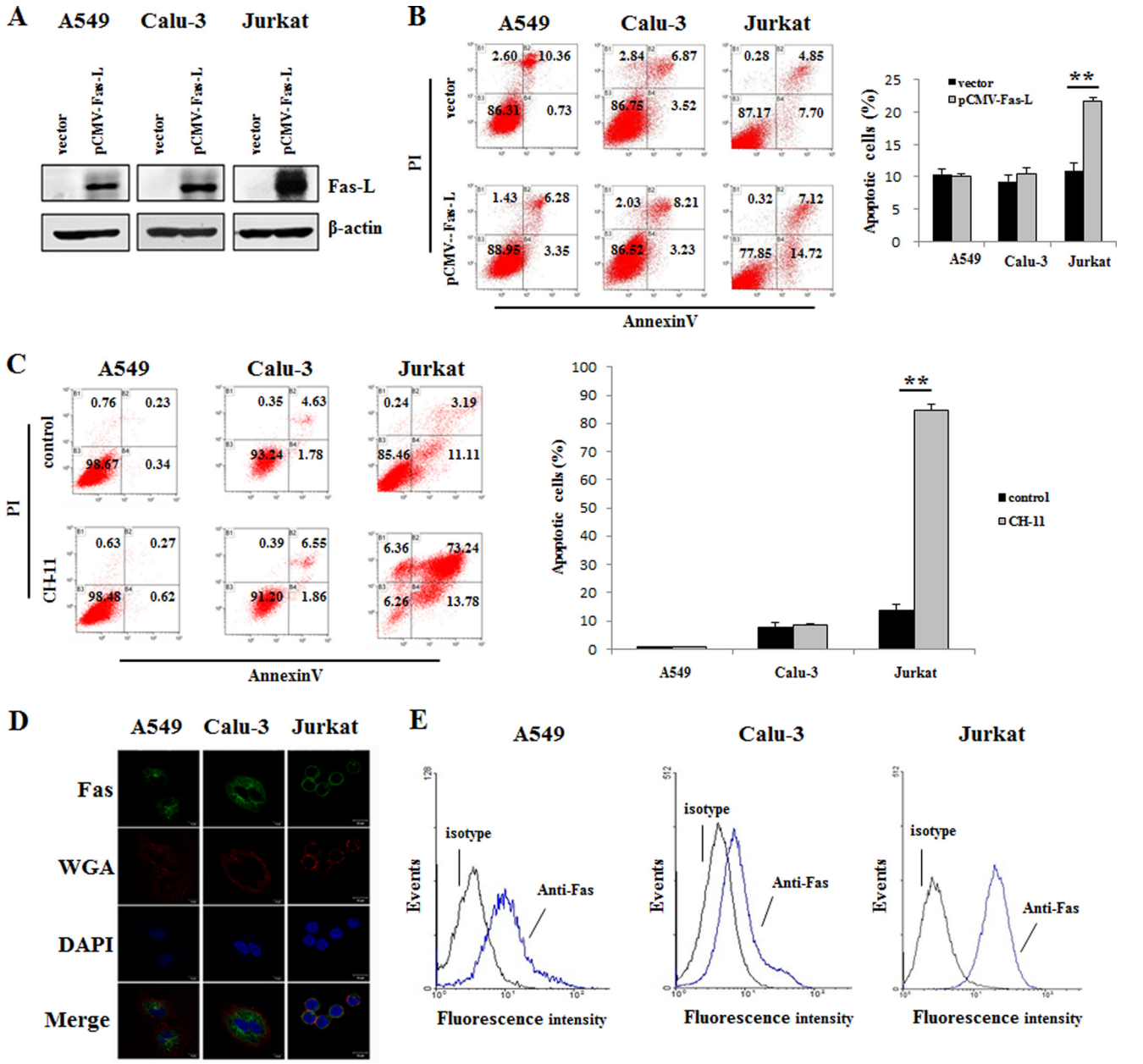


FIGURE 7. **The resistance of A549 and Calu-3 cells to Fas-L-induced apoptosis is due to the low level of cell surface Fas protein.** *A*, Western blot analysis of Fas-L production in A549, Calu-3, and Jurkat cells after transient transfection with the Fas-L gene for 48 h. *B* and *C*, effects of Fas-L overexpression (*B*) and anti-Fas antibody (CH-11, 5 $\mu$g/ml) (*C*) on apoptosis in A549, Calu-3, and Jurkat cells at 48 and 24 h after serum depletion, as evaluated by flow cytometry. The diagrams were derived from a representative experiment of three independent experiments. Quantification of the apoptotic cells is also shown. **, $p < 0.01$ *versus* the vector-only group. *PI*, propidium iodide. *D*, confocal microscopy of Fas protein in A549, Calu-3, and Jurkat cells using immunocytochemistry with anti-Fas antibody (*green*), WGA (*red*), and DAPI (*blue*). *Scale bar* = 10 $\mu$m. Data are representative of three independent experiments. *E*, surface Fas protein expression as measured by flow cytometry using FITC mouse IgG1 $\kappa$ isotype control (*isotype*) or FITC mouse anti-human CD95 (*Anti-Fas*). Data are representative of three independent experiments.

inhibition of FAP-1 protein expression that resulted from overexpressing PEDF (Fig. 9*E*). These data indicate that PEDF promoted plasma membrane Fas trafficking through the p53/FAP-1 axis.

*PPARγ Contributes to the Up-regulation of p53 by PEDF*—To further clarify the upstream regulator involved in the modulation of p53 by PEDF, the interrelations of PEDF, PPARγ, and p53 were investigated. We found that the overexpression of PEDF increased the PPARγ protein level (Fig. 10*A*). Knockdown of PPARγ diminished the up-regulation of p53 by PEDF (Fig. 10, *B* and *C*). Accordingly, the PEDF-induced increase of cell surface Fas was also inhibited by the silencing of PPARγ (Fig. 10*D*). These results suggest that PEDF up-regulated p53 via PPARγ.

## DISCUSSION

The Fas death signaling pathway plays an important role in tumorigenesis and is a widely studied target for cancer therapy. However, tumor cells have developed different mechanisms to evade Fas-mediated apoptosis (32). The down-regulation of cell surface Fas is frequently found in various tumor cells as one of the mechanisms for tumor cell non-responsiveness to apopto-

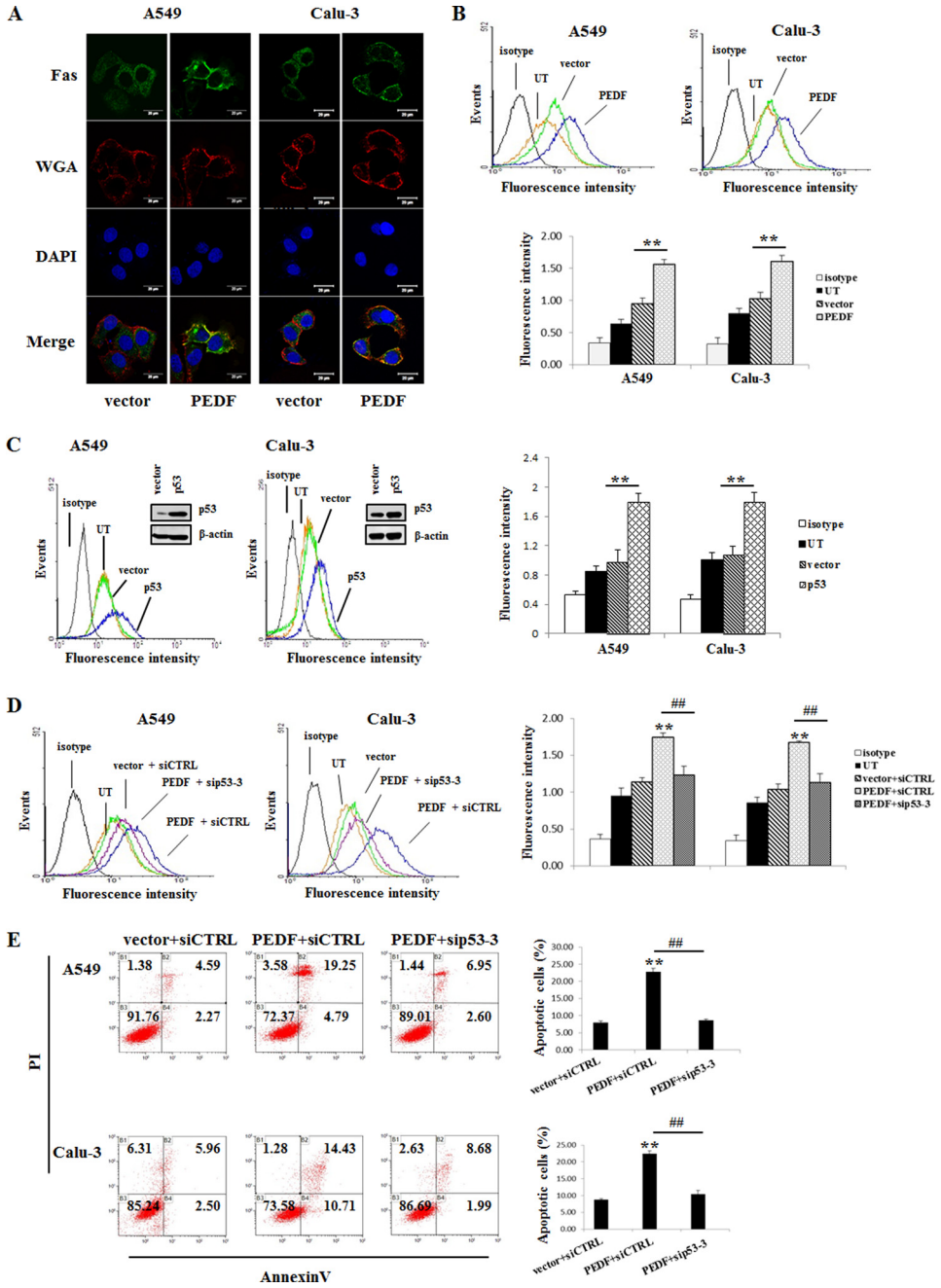


FIGURE 8. **PEDF up-regulates cell surface Fas via p53-mediated translocation.** *A*, confocal microscopy of the Fas immunofluorescence assays. Fluorescence images were acquired 48 h post-transfection of the PEDF gene after depletion of the serum. *Green*, Fas; red, WGA; *blue*, DAPI. Data are representative of three independent experiments. *B*, PEDF induced cell surface Fas as determined by flow cytometry. Representative histograms of three independent experiments are shown. The results are shown as mean ± S.D. of triplicates. **, $p < 0.01$ *versus* the vector-only group. *UT*, untreated group. *C*, cells were transfected with p53-pcDNA3.1 (+) for 48 h. Western blot analysis was performed to determine the protein levels of p53. Cell surface Fas was measured by flow cytometry. Representative histograms of three independent experiments are shown. The results are shown as mean ± S.D. of triplicates. **, $p < 0.01$ *versus* the vector-only group. *D* and *E*, knockdown of p53 was performed 24 h prior to the overexpression of PEDF. Cells were collected for cell surface Fas (*D*) and apoptosis evaluation (*E*) by flow cytometry. Representative flow cytometry histograms of three independent experiments are presented as above. Data are mean ± S.D. of triplicates. *siCTRL*, control siRNA. **, $p < 0.01$ *versus* vector + siCTRL group; ##, $p < 0.01$ *versus* PEDF + siCTRL group. *PI*, propidium iodide.

sis mediated by Fas (19). The data in this paper show that the lung cancer cell lines A549 and Calu-3 had low levels of cell surface Fas, whereas Jurkat cells had a high level of cell surface Fas. Because of this difference, A549 and Calu-3 cells were resistant to Fas-L- and CH-11-induced apoptosis. In contrast, the numbers of apoptotic cells were increased significantly increased by Fas-L overexpression and the treatment of CH-11 in Jurkat cells. These findings are supported by a previous study made by Nambu *et al.* (20) and suggest that some types of drugs might have potential for the treatment of lung cancer because of their ability to rescue the Fas death signaling pathway.

PEDF, originally theorized to be an angiogenesis inhibitor, has been reported to be able to directly target several types of tumor cells through inducing apoptosis (7–10). In this study, we showed that PEDF inhibited tumor growth and induced tumor cells apoptosis. However, this tumor cell apoptosis

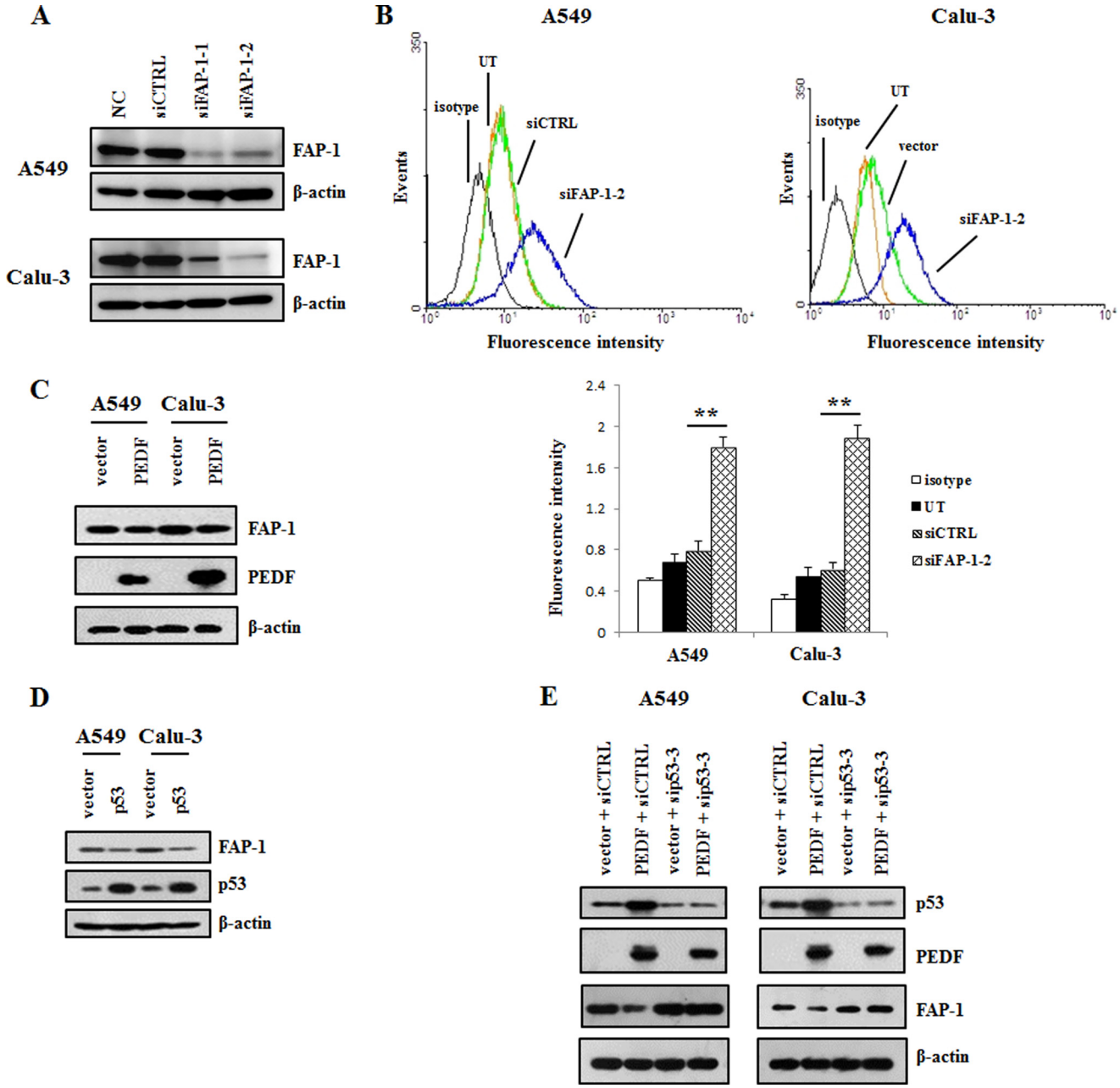


FIGURE 9. **FAP-1, a negative regulatory factor of cell surface Fas translocation, was decreased by PEDF via p53.** *A*, Western blotting analysis was employed to detect the protein levels of FAP-1 after the cells were transfected with siRNAs of FAP-1 for 48 h. The data are representative of three independent experiments. *NC,* normal control; *siCTRL*, control siRNA. *B*, plasma membrane Fas levels were determined by flow cytometry after the knockdown of FAP-1. Representative histograms from three independent experiments are shown. Data are mean ± S.D. **, $p < 0.01$ *versus* siCTRL group. *UT*, untreated group. *C* and *D*, Western blot analysis was used to evaluate the protein levels of FAP-1 following the overexpression of PEDF (*C*) or p53 (*D*). Data are representative of three independent experiments. *E*, cells were transfected with siRNA of p53 for 24 h prior to the transduction of PEDF-pcDNA3.1 (+). Next, the protein levels of FAP-1, p53, and PEDF were detected by Western blot analysis. Data are representative of three independent experiments.

might be due to nutrition deprivation resulting from the anti-angiogenesis activity of PEDF. We found that angiogenesis was repressed by PEDF in A549 xenografts. To confirm whether PEDF targets tumor cells *per se*, the lung cancer cell lines A549 and Calu-3 were exposed to rPEDF or transfected with the PEDF gene. The recombinant human endostatin injection (ENDOSTAR), a commercial antitumor drug used in the treatment of non-small cell lung cancer (NSCLC), was employed as a control to evaluate the efficacy of rPEDF. Although both recombinant proteins were obtained from *Escherichia coli*, rPEDF was more efficient than ENDOSTAR in targeting A549 cells. Additionally, rPEDF has been demonstrated to be more active than endostatin in antiangiogenesis (33). Therefore, PEDF might have a better efficacy in the treatment of NSCLC on the basis of its dual role in antitumor. Specially, we first reported that PEDF induced apoptosis of A549 and Calu-3 cells and led to activation of caspase 8, caspase 9, and PARP both *in vivo* and *in vitro*. By pretreatment with caspase 8/9 and caspase inhibitors, we demonstrated that PEDF-induced apoptosis was more extensively blocked by the caspase 8 inhibitor than by the caspase 9 inhibitor. Furthermore, knockdown of Fas-L protected A549 and Calu-3 cells from PEDF-induced apoptosis.

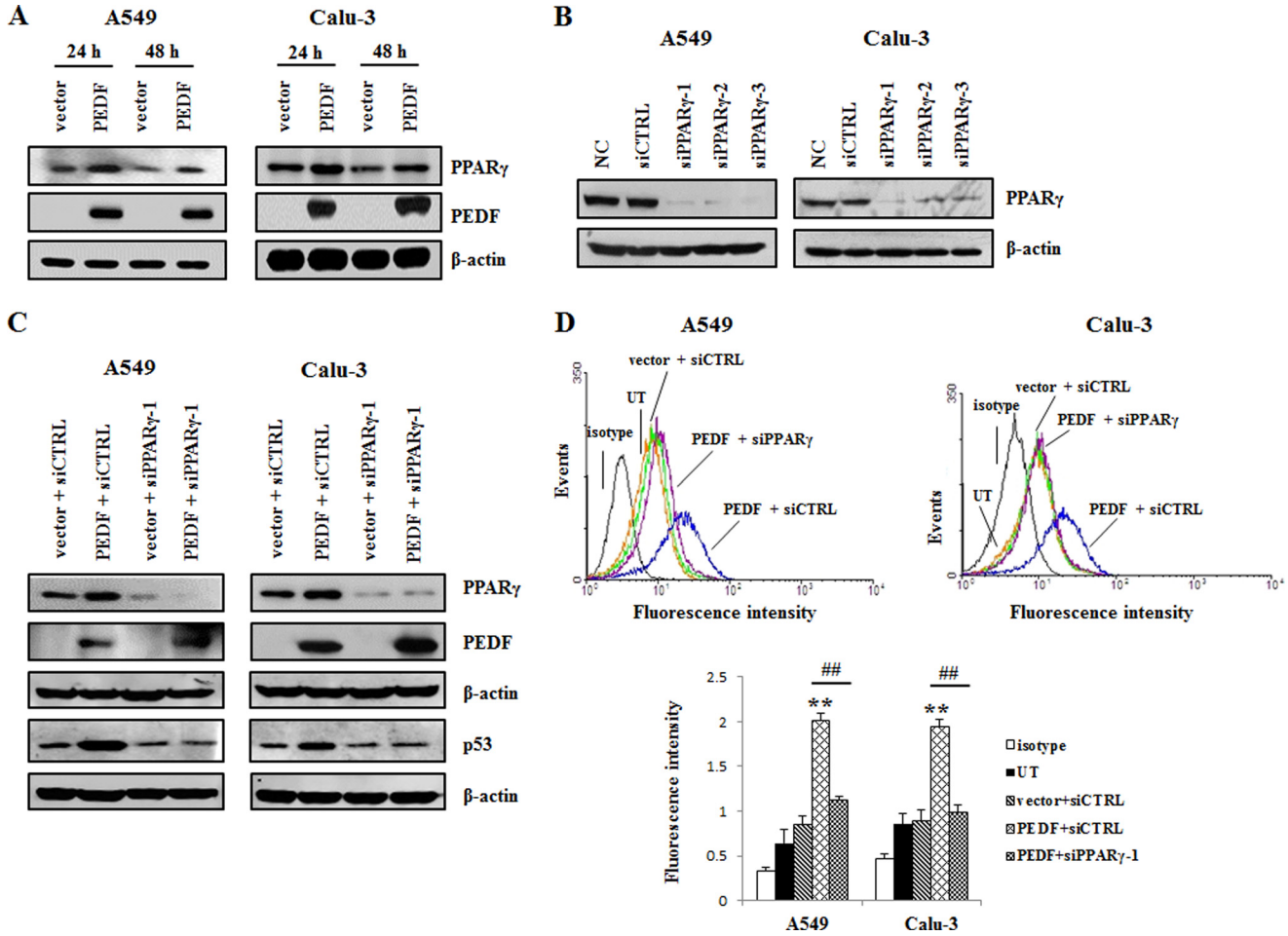


FIGURE 10. **PPARγ contributes to the up-regulation of p53 by PEDF.** *A*, cells were harvested after transfection with pcDNA3.1 (+) or PEDF-pcDNA3.1 (+) for 24 h and 48 h in the absence of serum. Next, the cells were subjected to Western blot analysis. The protein levels of PPARγ and PEDF were detected with PPARγ and PEDF antibodies, respectively. *B*, cells were transfected with PPARγ siRNAs (*siPPARγ-1/2/3*) or a nonspecific control siRNA (*siCTRL*) for 48 h. siRNA-mediated depletion of PPARγ was examined by Western blot analysis. *NC*, normal control. *C*, knockdown of PPARγ was performed 24 h prior to the overexpression of PEDF. Western blot analysis was used to determine the protein levels of p53, PEDF and PPARγ. *D*, in parallel experiments, flow cytometry was employed to measure cell surface Fas using FITC mouse anti-human CD95 (*Fas*). Representative flow cytometry histograms are presented as above. Data are mean ± S.D. **, $p < 0.01$ *versus* vector + siCTRL group; ##, $p < 0.01$ *versus* PEDF + iCTRL group. *UT*, untreated group. Data are representative of three independent experiments.

Therefore, it was interesting to find that the Fas-L/Fas/caspase 8 cascade was primarily involved in the PEDF-induced apoptosis of A549 and Calu-3 cells, whereas this cascade was corrupted as a result of the low level of plasma membrane Fas.

Increasing the surface display of Fas may be a key step to restore the Fas death signaling pathway and regain apoptotic ability for cells (15, 30, 34–39). A p53-responsive element has been found in the promoter of the human Fas gene (40). The translocation of p53 to the nucleus increased Fas expression under gefitinib-induced apoptosis (34). Another two studies have also shown that the induction of Fas expression was due to the activation of p53 by anticancer drugs. Furthermore, only wild-type p53 can transactivate the Fas gene because the protein level of Fas was not enhanced in cells with mutant p53 (35, 39). Clinical research in NSCLS has also confirmed that mutant p53 is related to negative Fas in samples (41). These findings suggest that increasing surface Fas through the transactivation of the Fas gene via wild- type p53 contributes to the apoptosis in Fas-deficient cells. The status of p53 in A549 cells has been identified as wild-type, whereas mutant p53 is found in Calu-3 cells (42). However, the mutant p53 in Calu-3 cells does not seem to compromise its functional activity (43). Alternatively, several studies have shown that p53 does not induce an increase of total Fas protein but remains to stimulate the cell surface Fas expression, which is ascribed to the promotion of the transport of Fas to cell surface by p53 (30, 37). Furthermore, PEDF has displayed its regulation ability of protein distribution by promoting the transfer of presenilin 1 from the perinuclear region to the cell membrane (44). In our study, we found that PEDF augmented cell surface Fas without an impact on overall Fas expression. Moreover, the overexpression of p53 also increased cell surface Fas, and PEDF up-regulated the expression of p53. The knockdown of p53 attenuated the PEDF-mediated up-regulation of cell surface Fas, which subsequently impeded PEDF-induced apoptosis in A549 and Calu-3 cells. These findings imply that p53 also took part in the repair of the Fas death signaling pathway that was initiated by PEDF in our study. In addition, the activated p53 might be involved in the cleavage of caspase 9, which was partly responsible for PEDF-induced apoptosis of lung cancer cells.

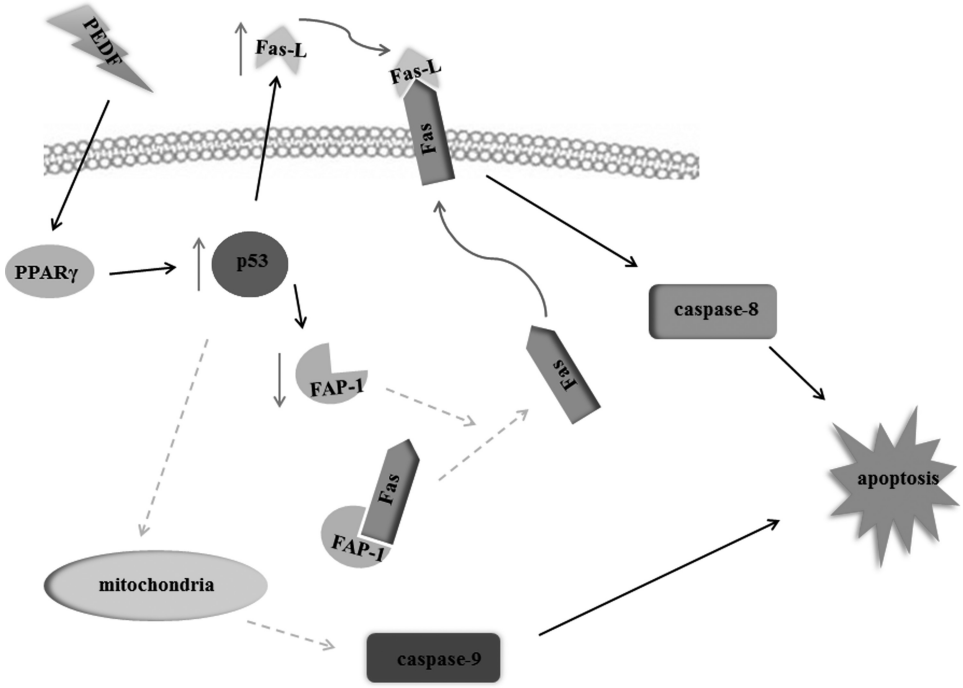


FIGURE 11. **Schematic of the underlying mechanism of PEDF-induced lung cancer cell apoptosis.** In the presence of PEDF, PPARγ is up-regulated, and then p53 is activated. The activation of p53, on one hand, up-regulates Fas-L expression. One the other hand, the activation of p53 down-regulates FAP-1 expression and the interaction between FAP-1 and Fas. The FAP-1-free Fas transports onto the cytoplasmic membrane and binds with the increased Fas-L, which activates caspase 8 and, therefore, induces cell apoptosis. In addition, the activation of p53 might also initiate the mitochondrial apoptotic pathway, promote the cleavage of caspase 9, and, finally, trigger cell apoptosis.

Fas (also known as CD95 or APO-1) belongs to the TNF receptor family and is a type I transmembrane protein (28) Therefore, it is well accepted that Fas ought to be present at the cell surface (45). As shown in Fig. 6*C*, the distribution of Fas in A549 and Calu-3 cells is nearly entirely limited to the cytoplasm. The Golgi apparatus has been reported to be the "chief culprit" in the intracellular sequestration of the Fas protein (30, 46). FAP-1 can bind to the last 15 amino acids in the C-terminal domain of Fas and colocalize with the Fas protein in the Golgi apparatus in pancreatic cancer cells. The association between FAP-1 and Fas inhibits the display of cell surface Fas (31). Tumor cells that possess elevated FAP-1 are largely refractory to Fas-mediated apoptosis (47). Consistent with these studies, we showed that knockdown of FAP-1 encouraged the cell surface display of Fas. Furthermore, the promoter of FAP-1 has been identified as a potential binding site for p53, and p53 activation suppresses the expression of FAP-1 (48, 49). We found similar results in that the overexpression of p53 reduced the protein level of FAP-1. The influence of PEDF on FAP-1 was eliminated by silencing p53. Therefore, the p53/FAP-1 axis is likely to explain the PEDF-induced export of Fas to the plasma membrane.

Fas-L is another target protein of anticancer drug-induced apoptosis. The increase of Fas-L protein might cause a sensitivity of tumor cells to anticancer drugs (35, 50). Here we demonstrated that PEDF led to the up-regulation of Fas-L both *in vivo* and *in vitro*. Wild-type p53 has been reported to mediate the activation of Fas-L (35, 51), and the up-regulation of p53 by PEDF is mediated by PPARγ (17). These reports suggest that the augmentation of the Fas-L protein might depend on the PPARγ/p53 cascade. However, in breast cancer cells, PPARγ has been shown to stimulate Fas-L expression by directly binding with its promoter (52). Here we observed that the up-regulation of Fas-L by PEDF in lung cancer cells was also mediated through the PPARγ/p53 cascade.

In summary, in addition to the antiangiogenic function of PEDF that has been described in our previous investigations (22, 53), this investigation showed that PEDF exerts a direct proapoptotic effect on lung cancer cells. The underlying mechanism of this process is delineated in Fig. 11. In particular, we are the first to show that a p53-mediated correction of the Fas death signaling pathway is engaged in the apoptotic process that is induced by PEDF. These findings provide strong evidence that the multifunctional endogenous factor PEDF is a promising drug for lung cancer therapy.

## REFERENCES

1. Steele, F. R., Chader, G. J., Johnson, L. V., and Tombran-Tink, J. (1993) Pigment epithelium-derived factor: neurotrophic activity and identification as a member of the serine protease inhibitor gene family. *Proc. Natl. Acad. Sci. U.S.A.* **90,** 1526–1530
2. Zhang, S. X., Wang, J. J., Gao, G., Shao, C., Mott, R., and Ma, J. X. (2006) Pigment epithelium-derived factor (PEDF) is an endogenous antiinflammatory factor. *FASEB J.* **20,** 323–325
3. Stellmach, V., Crawford, S. E., Zhou, W., and Bouck, N. (2001) Prevention of ischemia-induced retinopathy by the natural ocular antiangiogenic agent pigment epithelium-derived factor. *Proc. Natl. Acad. Sci. U.S.A.* **98,** 2593–2597
4. Crowe, S., Wu, L. E., Economou, C., Turpin, S. M., Matzaris, M., Hoehn, K. L., Hevener, A. L., James, D. E., Duh, E. J., and Watt, M. J. (2009) Pigment epithelium-derived factor contributes to insulin resistance in obesity. *Cell Metab.* **10,** 40–47
5. Ek, E. T., Dass, C. R., and Choong, P. F. (2006) Pigment epithelium-derived factor: a multimodal tumor inhibitor. *Mol. Cancer Ther.* **5,** 1641–1646
6. Broadhead, M. L., Dass, C. R., and Choong, P. F. (2009) *In vitro* and *in vivo*

biological activity of PEDF against a range of tumors. *Expert Opin. Ther. Targets* **13,** 1429–1438
7. Guan, M., Jiang, H., Xu, C., Xu, R., Chen, Z., and Lu, Y. (2007) Adenovirus-mediated PEDF expression inhibits prostate cancer cell growth and results in augmented expression of PAI-2. *Cancer Biol. Ther.* **6,** 419–425
8. Guan, M., Pang, C. P., Yam, H. F., Cheung, K. F., Liu, W. W., and Lu, Y. (2004) Inhibition of glioma invasion by overexpression of pigment epithelium-derived factor. *Cancer Gene Ther.* **11,** 325–332
9. Abe, R., Shimizu, T., Yamagishi, S., Shibaki, A., Amano, S., Inagaki, Y., Watanabe, H., Sugawara, H., Nakamura, H., Takeuchi, M., Imaizumi, T., and Shimizu, H. (2004) Overexpression of pigment epithelium-derived factor decreases angiogenesis and inhibits the growth of human malignant melanoma cells *in vivo*. *Am. J. Pathol.* **164,** 1225–1232
10. Ek, E. T., Dass, C. R., Contreras, K. G., and Choong, P. F. (2007) Pigment epithelium-derived factor overexpression inhibits orthotopic osteosarcoma growth, angiogenesis and metastasis. *Cancer Gene Ther.* **14,** 616–626
11. Chen, J. F., Zhao, W., Zhang, J. Z., Jiang, W. G., and Zhang, L. J. (2009) Effects of pigment epithelial derived factor gene on growth of lung cancer cell and neovascularization: experiments with lung cancer cells and chick embryos. *Zhonghua Yi Xue Za Zhi* **89,** 485–490
12. He, S. S., Shi, H. S., Yin, T., Li, Y. X., Luo, S. T., Wu, Q. J., Lu, L., Wei, Y. Q., and Yang, L. (2012) AAV-mediated gene transfer of human pigment epithelium-derived factor inhibits Lewis lung carcinoma growth in mice. *Oncol. Rep.* **27,** 1142–1148
13. Chen, J., Ye, L., Zhang, L., and Jiang, W. G. (2009) The molecular impact of pigment epithelium-derived factor, PEDF, on lung cancer cells and the clinical significance. *Int. J. Oncol.* **35,** 159–166
14. Peter, M. E., Legembre, P., and Barnhart, B. C. (2005) Does CD95 have tumor promoting activities? *Biochim. Biophys. Acta* **1755,** 25–36
15. Volpert, O. V., Zaichuk, T., Zhou, W., Reiher, F., Ferguson, T. A., Stuart, P. M., Amin, M., Bouck, N. P. (2002) Inducer-stimulated Fas targets activated endothelium for destruction by anti-angiogenic thrombospondin-1 and pigment epithelium-derived factor. *Nat. Med.* **8,** 349–357
16. Ho, T. C., Chen, S. L., Yang, Y. C., Lo, T. H., Hsieh, J. W., Cheng, H. C., and Tsao, Y. P. (2009) Cytosolic phospholipase A2-$\alpha$ is an early apoptotic activator in PEDF-induced endothelial cell apoptosis. *Am. J. Physiol. Cell Physiol.* **296,** C273–C284
17. Ho, T. C., Chen, S. L., Yang, Y. C., Liao, C. L., Cheng, H. C., and Tsao, Y. P. (2007) PEDF induces p53-mediated apoptosis through PPAR $\gamma$ signaling in human umbilical vein endothelial cells. *Cardiovasc. Res.* **76,** 213–223
18. Müschen, M., Warskulat, U., and Beckmann, M. W. (2000) Defining CD95 as a tumor suppressor gene. *J. Mol. Med.* **78,** 312–325
19. Owen-Schaub, L. B., Radinsky, R., Kruzel, E., Berry, K., and Yonehara, S. (1994) Anti-Fas on nonhematopoietic tumors: levels of Fas/APO-1 and bcl-2 are not predictive of biological responsiveness. *Cancer Res.* **54,** 1580–1586
20. Nambu, Y., Hughes, S. J., Rehemtulla, A., Hamstra, D., Orringer, M. B., and Beer, D. G. (1998) Lack of cell surface Fas/APO-1 expression in pulmonary adenocarcinomas. *J. Clin. Invest.* **101,** 1102–1110
21. Viard-Leveugle, I., Veyrenc, S., French, L. E., Brambilla, C., and Brambilla, E. (2003) Frequent loss of Fas expression and function in human lung tumours with overexpression of FasL in small cell lung carcinoma. *J. Pathol.* **201,** 268–277
22. Yang, H., Cheng, R., Liu, G., Zhong, Q., Li, C., Cai, W., Yang, Z., Ma, J., Yang, X., and Gao, G. (2009) PEDF inhibits growth of retinoblastoma by anti-angiogenic activity. *Cancer Sci.* **100,** 2419–2425
23. Lin, C. S., Xie, S. B., Liu, J., Zhao, Z. X., Chong, Y. T., and Gao, Z. L. (2010) Effect of revaccination using different schemes among adults with low or undetectable anti-HBs titers after hepatitis B virus vaccination. *Clin. Vaccine Immunol.* **17,** 1548–1551
24. Zheng, J., Jiang, H. Y., Li, J., Tang, H. C., Zhang, X. M., Wang, X. R., Du, J. T., Li, H. B., and Xu, G. (2012) MicroRNA-23b promotes tolerogenic properties of dendritic cells *in vitro* through inhibiting Notch1/NF-$\kappa$B signalling pathways. *Allergy* **67,** 362–370
25. Xu, G., Cheng, L., Wen, W., Oh, Y., Mou, Z., Shi, J., Xu, R., Li, H. (2007) Inverse association between T-cell immunoglobulin and mucin domain-1 and T-bet in a mouse model of allergic rhinitis. *Laryngoscope* **117,** 960–964
26. Weidner, N., Semple, J. P., Welch, W. R., and Folkman, J. (1991) Tumor angiogenesis and metastasis: correlation in invasive breast carcinoma. *N. Engl. J. Med.* **324,** 1–8
27. Chen, M., and Wang, J. (2002) Initiator caspases in apoptosis signaling pathways. *Apoptosis* **7,** 313–319
28. Ehrenschwender, M., and Wajant, H. (2009) The role of FasL and Fas in health and disease. *Adv. Exp. Med. Biol.* **647,** 64–93
29. Kawasaki, M., Kuwano, K., Nakanishi, Y., Hagimoto, N., Takayama, K., Pei, X. H., Maeyama, T., Yoshimi, M., and Hara, N. (2000) Analysis of Fas and Fas ligand expression and function in lung cancer cell lines. *Eur. J. Cancer* **36,** 656–663
30. Bennett, M., Macdonald, K., Chan, S. W., Luzio, J. P., Simari, R., and Weissberg, P. (1998) Cell surface trafficking of Fas: a rapid mechanism of p53-mediated apoptosis. *Science* **282,** 290–293
31. Ungefroren, H., Kruse, M. L., Trauzold, A., Roeschmann, S., Roeder, C., Arlt, A., Henne-Bruns, D., and Kalthoff, H. (2001) FAP-1 in pancreatic cancer cells: functional and mechanistic studies on its inhibitory role in CD95-mediated apoptosis. *J. Cell Sci.* **114,** 2735–2746
32. Villa-Morales, M., and Fernández-Piqueras J. (2012) Targeting the Fas/FasL signaling pathway in cancer therapy. *Expert Opin. Ther. Targets* **16,** 85–101
33. Dawson, D. W., Volpert, O. V., Gillis, P., Crawford, S. E., Xu, H., Benedict, W., and Bouck, N. P. (1999) Pigment epithelium-derived factor: a potent inhibitor of angiogenesis. *Science* **285,** 245–248
34. Rho, J. K., Choi, Y. J., Ryoo, B. Y., Na, I. I., Yang, S. H., Kim, C. H., Lee, J. C. (2007). p53 enhances gefitinib-induced growth inhibition and apoptosis by regulation of Fas in non-small cell lung cancer. *Cancer Res.* **67,** 1163–1169
35. Müller, M., Strand, S., Hug, H., Heinemann, E. M., Walczak, H., Hofmann, W. J., Stremmel, W., Krammer, P. H., and Galle, P. R. (1997) Drug-induced apoptosis in hepatoma cells is mediated by the CD95 (APO-1/Fas) receptor/ligand system and involves activation of wild-type p53. *J. Clin. Invest.* **99,** 403–413
36. Sodeman, T., Bronk, S. F., Roberts, P. J., Miyoshi, H., and Gores, G. J. (2000) Bile salts mediate hepatocyte apoptosis by increasing cell surface trafficking of Fas. *Am. J. Physiol. Gastrointest. Liver Physiol.* **278,** G992–G999
37. Beltinger, C., Fulda, S., Kammertoens, T., Meyer, E., Uckert, W., and Debatin, K. M. (1999) Herpes simplex virus thymidine kinase/ganciclovir-induced apoptosis involves ligand-independent death receptor aggregation and activation of caspases. *Proc. Natl. Acad. Sci. U.S.A.* **96,** 8699–8704
38. Weller, M., Malipiero, U., Rensing-Ehl, A., Barr, P. J., and Fontana, A. (1995) Fas/APO-1 gene transfer for human malignant glioma. *Cancer Res.* **55,** 2936–2944
39. Müller, M., Wilder, S., Bannasch, D., Israeli, D., Lehlbach, K., Li-Weber, M., Friedman, S. L., Galle, P. R., Stremmel, W., Oren, M., Krammer, P. H. (1998) p53 activates the CD95 (APO-1/Fas) gene in response to DNA damage by anticancer drugs. *J. Exp. Med.* **188,** 2033–2045
40. Munsch, D., Watanabe-Fukunaga, R., Bourdon, J. C., Nagata, S., May, E., Yonish-Rouach, E., and Reisdorf, P. (2000) Human and mouse Fas (APO-1/CD95) death receptor genes each contain a p53-responsive element that is activated by p53 mutants unable to induce apoptosis. *J. Biol. Chem.* **275,** 3867–3872
41. Lee, S. H., Shin, M. S., Park, W. S., Kim, S. Y., Kim, H. S., Han, J. Y., Park, G. S., Dong, S. M., Pi, J. H., Kim, C. S., Kim, S. H., Lee, J. Y., and Yoo, N. J. (1999) Alterations of Fas (Apo-1/CD95) gene in non-small cell lung cancer. *Oncogene* **18,** 3754–3760
42. Pratesi, G., Perego, P., Polizzi, D., Righetti, S. C., Supino, R., Caserini, C., Manzotti, C., Giuliani, F. C., Pezzoni, G., Tognella, S., Spinelli, S., Farrell, N., and Zunino, F. (1999) A novel charged trinuclear platinum complex effective against cisplatin-resistant tumours: hypersensitivity of p53-mutant human tumour xenografts. *Br. J. Cancer* **80,** 1912–1919
43. Buqué, A., Muhialdin, J. Sh., Muñoz, A., Calvo, B., Carrera, S., Aresti, U., Sancho, A., Rubio, I., and López-Vivanco, G. (2012) Molecular mechanism implicated in Pemetrexed-induced apoptosis in human melanoma cells. *Mol. Cancer* **11,** 25
44. Cai, J., Jiang, W. G., Grant, M. B., and Boulton, M. (2006) Pigment epithe-

lium-derived factor inhibits angiogenesis via regulated intracellular proteolysis of vascular endothelial growth factor receptor 1. *J. Biol. Chem.* **281,** 3604–3613
45. Siegel, R. M., Frederiksen, J. K., Zacharias, D. A., Chan, F. K., Johnson, M., Lynch, D., Tsien, R. Y., and Lenardo, M. J. (2000) Fas preassociation required for apoptosis signaling and dominant inhibition by pathogenic mutations. *Science* **288,** 2354–2357
46. Haynes, A. P., Daniels, I., Abhulayha, A. M., Carter, G. I., Metheringham, R., Gregory, C. D., and Thomson, B. J. (2002) CD95 (Fas) expression is regulated by sequestration in the Golgi complex in B-cell lymphoma. *Br. J. Haematol.* **118,** 488–494
47. Ivanov, V. N., Lopez Bergani, P., Maulit, G., Sato, T. A., Sassoon, D., and Ronai, Z. (2003) FAP-1 association with Fas (Apo-1) inhibits Fas expression on the cell surface. *Mol. Cell Biol.* **23,** 3623–3635
48. Yamada, T., Maruyama, M., Fujita, T., Miyabayashi, K., Shinoda, C., Kawagishi, Y., Fujishita, T., Hayashi, R., Miwa, T., Arai, N., Matsui, S., Sugiyama, E., and Kobayashi, M. (2006) Ionizing radiation suppresses FAP-1 mRNA level in A549 cells via p53 activation. *FEBS Lett.* **580,** 4387–4391
49. Irie, S., Li, Y., Kanki, H., Ohyama, T., Deaven, L. L., Somlo, S., and Sato, T. A. (2001) Identification of two Fas-associated phosphatase-1 (FAP-1) promoters in human cancer cells. *DNA Seq.* **11,** 519–526
50. Friesen, C., Herr, I., Krammer, P. H., and Debatin, K. M. (1996) Involvement of the CD95 (APO-1/FAS) receptor/ligand system in drug-induced apoptosis in leukemia cells. *Nat. Med.* **2,** 574–577
51. Roy, J., Pallepati, P., Bettaieb, A., and Averill-Bates, D. A. (2010) Acrolein induces apoptosis through the death receptor pathway in A549 lung cells: role of p53. *Can J. Physiol. Pharmacol.* **88,** 353–368
52. Bonofiglio, D., Gabriele, S., Aquila, S., Qi, H., Belmonte, M., Catalano, S., and Andò, S. (2009) Peroxisome proliferator-activated receptor γ activates fas ligand gene promoter inducing apoptosis in human breast cancer cells. *Breast Cancer Res. Treat* **113,** 423–434
53. Li, L., Yang, J., Wang, W. W., Yao, Y. C., Fang, S. H., Dai, Z. Y., Hong, H. H., Yang, X., Shuai, X. T., and Gao, G. Q. (2012) Pigment epithelium-derived factor gene loaded in cRGD-PEG-PEI suppresses colorectal cancer growth by targeting endothelial cells. *Int. J. Pharm.* **438,** 1–10